

Kinetic Behavior of Immobilized Tyrosinase on Carbon in a Simulated Packed-Bed Reactor

Sun Kyoung Shin, Kyeo-Keun Kim*

Dept. of Environ. Health Res., Nat'l Inst. of Environ. Res., 122-040 Seoul, Korea

*Dept. of Environ. Eng., Chongju Univ., Chongju 360-764, Korea

(Received Aug. 1, 1996)

충전층에서 탄소에 고정시킨 Tyrosinase의 반응속도에 관한 연구

신선경 · 김교근*

국립환경연구원 환경보건부 미량물질분석과

*청주대학교 이공대학 환경공학과

(1996. 8. 1. 접수)

Abstract : Influence of the axial dispersion on immobilized enzyme catalytic bed was investigated in order to examine the kinetic behavior of the biocatalysis. The enzyme employed in this study was the tyrosinase(EC 1.14.18.1) immobilized on carbon support : this system requires two substrates of phenol and oxygen. This enzyme has potential application for phenol degradation in waste water. A simulated reactor was a packed-bed reactor of 2.54cm in diameter and 10cm long, loaded with the immobilized carbon particle with an average diameter of 550 μ m. A phenol feed in the strength of 55.5mM(5220ppm) was used to observe the behavior of the immobilized enzyme column at three different dissolved oxygen levels of 0.08445mM(2.7ppm), 0.1689mM(5.4ppm) and 0.3378mM(9.5ppm) with the flow rates in the range of 60(1mL/s) to 180mL/min(3mL/s).

Examination of the Biot number and Damkolher numbers of the immobilized system enables us to eliminate the contribution of external mass transfer to set of differential equations derived from the dispersion model. Solution of the equation was finally obtained numerically with the application of the Danckwert boundary conditions and the assumed zero- and first order rates on the non-linear two substrate enzyme kinetics. Higher conversion of phenol was observed at the low flow rates and at the higher oxygen concentration.

Comparison of axial dispersion and plug flow model showed that no detectable difference was observed in the column outlet conversion between the axial and the plug flow models which was in complete agreement with the previous studies.

요약 : 지름 2.54cm, 길이 10cm인 유리관에 tyrosinase(EC. 1.14.18.1)를 입자의 크기 550 μ m 인 탄소에 고정시켜 충전하고, 페놀과 산소를 기질로 사용하여 tyrosinase의 반응 특성을 조사하기 위해 axial dispersion 모델을 제안하였다. 본 논문에서 페놀의 농도는 55.5mM로 고정시키고 산소(2.7ppm, 5.4ppm, 그리고 9.5ppm)와 유속 (1~3mL/s)을 변화시키면서 탄소에 고정된 tyrosinase의 반응을 관찰하였다. 또한, Damkolher수를 계산하고 분산 특성과 식으로부터 효소 반응 속도 및 분산의 영향을 예측하기 위해 수치적 해석을 하였다.

연구 결과 물질저항은 주로 외부 전달과 내부확산이었으며, 제안된 모델에서 Biot수는 64.25였다. 펄스는 1.0mL/s 정도의 느린 속도에서 산소의 농도가 높을수록 높은 전환율을 나타내었다. 한편, axial dispersion 모델과 plug flow 모델의 비교에서는 모두 같은 전환율을 나타내어 axial dispersion 모델이 반응속도와 무관함을 알 수 있었다.

Key words : axial dispersion, immobilized enzyme, tyrosinase, phenol, kinetics.

1. Introduction

The immobilized tyrosinase(monophenol oxidase, EC 1.14.18.1) have been employed in a packed-bed reactor to degrade phenol to quinone. The several factors need to be considered; the change of the enzymes properties resulted from immobilization and the factors related to the chemical reaction with mass transfer resistance. The tyrosinase contains a copper ion and oxidizes the phenols into melanin after successive two enzymatic steps. The two sequential reaction steps were reported to be involved in the oxidation of phenols.¹⁻⁴ The first reaction is hydroxylation of monophenols to *ortho*-diphenols, and the second reaction is oxidation of *ortho*-diphenol to *ortho*-quinone. In both reactions molecular oxygen is required but it appears that the mechanisms are quite different from the mechanisms involved with the glucose oxidase which belong to the same enzyme classification. *ortho*-Quinone, the product of the enzymic reaction, is generally an unstable compound in an aqueous reaction medium, and must go through a set of chemical reactions that lead to other more stable compounds.

The purpose of this investigation is to study the kinetic behavior of immobilized tyrosinase in a simulated packed-bed reactor. The free enzyme will be assumed to have been successfully immobilized on activated carbon particles and follows the two-substrate enzyme kinetics. Since one of the substrates is a gaseous component (air), it may cause significant dispersive effects in both the radial and axial directions. Only the axial direction was considered

in this study. A mechanical model was developed based on the dispersion model and the internal and external transfer resistances. The rate equations from the model were solved numerically.

2. Theory

The tyrosinase, like many other oxidoreductase, required two substrates : phenol(or tyrosine) and oxygen. Because of the requirement of the two substrates, a number of different reaction mechanisms were proposed.¹⁻⁴ The schematic diagrams of these

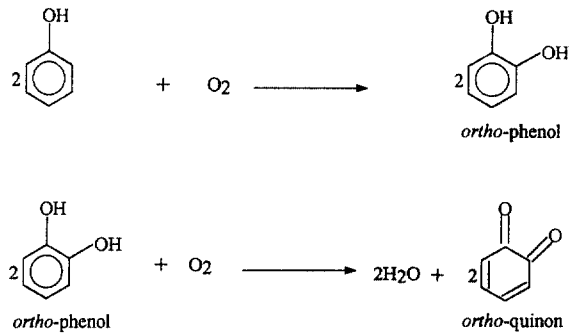


Fig. 1. Schematic diagram of mechanism 1.

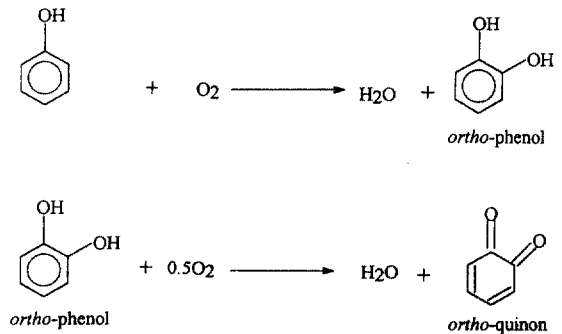
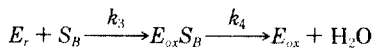
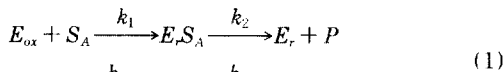


Fig. 2. Schematic diagram of mechanism 2.

two mechanisms are presented in Fig. 1 and 2. In the mechanism 1, the first step is the *ortho*-hydroxylation of monophenols to produce *ortho*-diphenol, and, in the second step, the dehydrogenation of *ortho*-dihydroxyphenols to form *ortho*-quinone. As noted in these diagrams, molecular oxygen is required in both reaction. According to a previous study⁵, irreversible inactivation of the enzyme were reported to be found during the oxidation of *ortho*-diphenols to *ortho*-quinone, the second reaction step. From the diagrams it is clear that the second mechanism is eventually the same as the first, except a different stoichiometric amount of oxygen is consumed in each step.

Because of consecutive steps of the reaction scheme, several possible kinetic models are to be considered in order to find a proper kinetic expression for phenol degradation.⁶⁻⁹ Regardless of these models, the kinetic study of phenol oxidation by tyrosinase has not been made in detail yet. Therefore, in this theoretical study, the enzyme kinetic expression was selected as the following.⁷



$$R_T = \frac{V_m S_A S_B}{A S_A S_B + B S_B + C S_A} \quad (2)$$

where, E_{ox} and E_r represent the fully oxidized form and the fully reduced form of an enzyme and

$$V_m = k_2 e_0, A = \frac{k_2 + k_4}{k_4}, B = \frac{k_2}{k_1}, C = \frac{k_2}{k_3}$$

3. Development of theoretical model

3.1. Enzyme kinetic

In the presence of an excess amount of one of the substrates, the rate expression of equation (2) becomes

$$R_T = \frac{V_m^* S_B}{K_m^* + S_B} \quad (3)$$

$$\text{where, } \frac{1}{V_m^*} = \frac{1}{k_1 e_0} \frac{1}{S_A} + \frac{k_2 + k_4}{k_2 k_4} \frac{1}{e_0}$$

$$\frac{1}{K_m^*} = \frac{k_3}{k_1} \frac{1}{S_A} + \frac{k_3(k_2 + k_4)}{k_2 k_4}$$

Here K_m^* is a modified Michaelis-Menten constant, and V_m^* is a revised maximum reaction rate per unit volume of the porous material. The V_m^* is dependent on total enzyme concentration, whereas the K_m^* is not. Once the assumption of excess amount of phenol is imposed, the equation (3) would become the form of the simple Michaelis-Menten kinetic equation with modified constants.

3.2. Kinetic study of the immobilized tyrosinase on activated carbon

In this study, only the axial dispersion was considered. This implication is valid whenever there is relatively low flow rate of the liquid in a packed column. Most of the enzymatic reactions are considered mild. Therefore, it is isothermal and the heat generation can be neglected. For this reason the energy balance equation can be eliminated. With the radial dispersion neglected, the following equation (5) is obtained as a reduced form of the dispersion model equation at steady state condition.

$$V_f \frac{\partial S}{\partial t} = V_f D_{fz} \frac{\partial^2 S}{\partial z^2} - V_f u_r \frac{\partial S}{\partial z} + \frac{V_f D_r}{r} \frac{\partial}{\partial r} \left(r \frac{\partial S}{\partial r} \right) - V_s R_T(S, T) \quad (4)$$

$$D_{fc} \frac{d^2 S_B}{dz^2} - u_s \frac{dS_B}{dz} - (1 - \epsilon) R_T(S_B) = 0 \quad (5)$$

where, V_f = fluid volume, V_s = solid catalyst volume, S = reactants concentration in fluid, D_{fz} = fluid axial mass dispersion coefficient, D_{fr} = fluid

radial mass dispersion coefficient, u_i = fluid interstitial velocity, z = axial coordinate, r = radial coordinate, $R(S, T)$ = rate of reaction in a catalyst pellet based on the bulk concentration and temperature, $D_{e,z}$ = effective dispersion coefficients in the axial dispersion ($\epsilon D_{i,z}$) and u_s = superficial velocity (ϵu_i).

The following equation is obtained through combining equation (3) and (5) by introducing the dimensionless concentration (S) and position (λ)

$$\frac{1}{Pe} \frac{d^2 S}{d\lambda^2} - \frac{dS}{d\lambda} - (1 - \epsilon) Da \frac{S_{B0} S}{K_m^0 + S_{B0} S} = 0 \quad (6)$$

where,

$$R_T = \eta \frac{V_m^* S_B}{K_m^* + S_B} = \frac{V_m^i S_B}{K_m^i + S_B}, S = \frac{S_B}{S_{B0}},$$

$$\lambda = \frac{z}{L}, Pe = \frac{u_s L}{D_{e,z}}, Da = \frac{LV_m^i}{u_s S_{B0}}$$

This equation is solved with the boundary conditions.

$$\text{at } \lambda = 0, S - \frac{1}{Pe} \frac{dS}{d\lambda} = 1 \quad (7)$$

$$\text{at } \lambda = 1, \frac{dS}{d\lambda} = 0$$

3.3 Immobilization of tyrosinase on activated carbon

Tyrosinase was immobilized onto activated carbon as follows. A known amount of activated carbon was soaked in the tyrosinase solution, 6mg/mL, at 4°C for 24 hr to allow for the enzyme penetration into the porous structure. The particles were then separated from the solution and rinsed thoroughly with distilled water. The rinsed carbon was added to 100mL of 0.5% glutaraldehyde for overnight cross-linking. The tyrosinase activity and stability increased following the paper.¹⁰

4. Results and discussion

4.1. External mass transfer resistance in the reactor

The parameter and conditions employed for a simulated enzyme reactor are listed in Table 1. A packed bed reactor, 10cm short and 2.54cm diameter, was selected because the reactor is presently used in our laboratory as a model reactor for the immobilized tyrosinase. The reactor was jacketed to maintain constant temperature. For the carbon support, the selected particle diameter of 550µm was a typical size for a supporting material for any

Table 1. Reactor parameters and constants

Parameters and constants	value	unit
reactor radius, R	0.0127	m
reactor length, L	0.10	m
void fraction of reactor volume, ϵ	0.35	
inlet concentration of oxygen, S_{B0}	0.1689	mM
density of fluid	997.80	kg/m ³
viscosity of fluid	0.8937	kg/m · s
particle diameter, D_p	5.50×10^{-4}	m
*Michaelis-Menten constant, K_m^i	0.169	mM
*maximum reaction rate, K_m^0	1.324	mM/min.

*These parameters are from the reference[10]. Coupled with the appropriate boundary conditions are obtained for the enzyme under the assumption of rate, K_m^0 .

Table 2. Calculated mass transfer coefficients

flow rate (mL/s)	mass transfer coefficient ($k_c \times 10^4$ m/s)	Reynolds number Re
1.00	1.044	1.211
1.25	1.124	1.512
1.50	1.195	1.816
1.75	1.257	2.117
2.00	1.315	2.422
2.25	1.368	2.729
2.50	1.416	3.028
2.75	1.462	3.330
3.00	1.508	3.633

enzyme. Two apparent constants V_m^i and K_m^i were obtained from the previously reported values.¹⁰ The flow rates ranging from 1 to 3 mL/s were used in this study and were presented in Table 2. These flow rates represented the actual flow of the liquid through the column, without causing significant pressure drop. The phenol concentrations of 55.5 mM in aqueous solution was used.

In order to justify the assumption on the excess amount of phenol over the dissolved oxygen, the solubility data for the oxygen in water was taken from literature¹¹ and compared with the phenol concentration. By comparing the phenol concentration of 55.5 mM which is commonly found in a wastewater with that of the saturated oxygen concentration of 0.1689 mM at 25°C the phenol concentration is about 300 times higher than the counterpart, thus, assuring the excess amount of phenol present during the reaction.

The mass transfer coefficients for the flow rates, k_c , were estimated from the Colburn J_D factors.¹² The estimated values of k_c at the different flow rates are shown in Table 2. There were also several other procedures for estimating the mass transfer coefficients including the graphical method and empirical correlating equations.

The typical Biot number for the carbon particle was found to be 64.25 at the flow rate 1.5 mL/s, which was considerably larger than reported number. By comparing the Biot number of 64.25 and the experimental finding by Goldstein and Manecke¹³ (the external mass transfer limitation became negligible for Biot numbers over 50), it can be concluded that the external mass transfer resistance has a negligible effect.

4.2. Axial dispersion in the reactor

The concentration profiles of oxygen as a function of the reactor length were obtained through computer program, and the results of the computation are presented in Fig. 3, 4 and 5. The dimensionless concentration profiles and length were

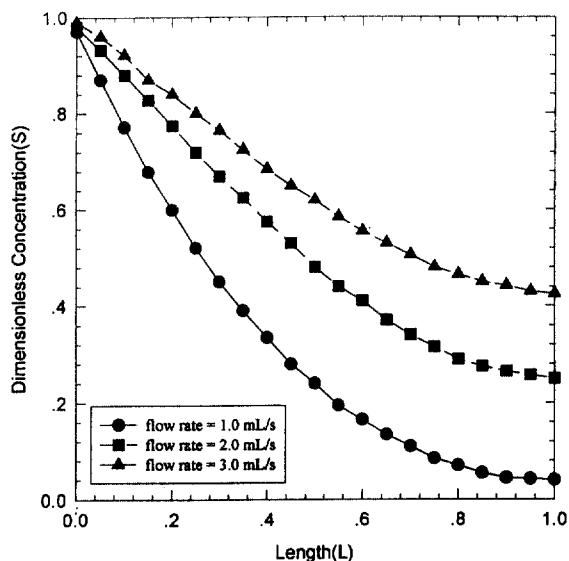


Fig. 3. Plot of the dimensionless concentration profile versus length at three different flow rate.

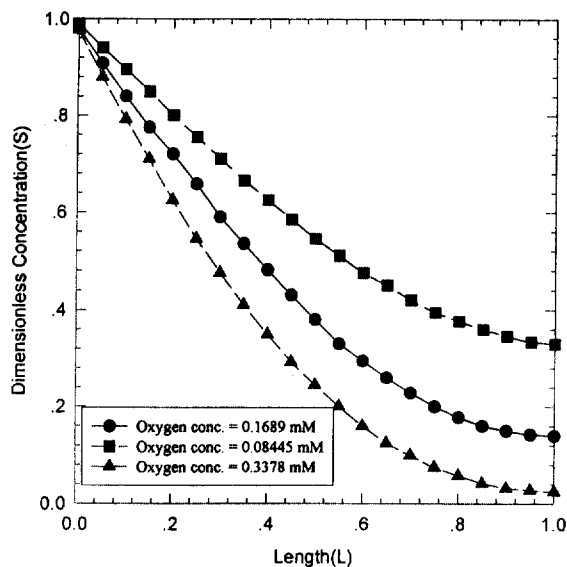


Fig. 4. The change of oxygen concentration along the length of catalytic bed (flow rate = 1.5 mL/s).

used in the figures. In Fig. 3, at the relatively low flow rate of 1.00 mL/s, the dimensionless oxygen concentration was 0.03880 at the end of the reactor, while, at the relatively high flow rate of 3.00 mL/s, this value showed 0.4281. The corresponding oxygen conversions are 0.9612 (96.12%) for 1 mL/s, and 0.

5782(57.82%) for 3mL/s suggesting that the conversion of oxygen is unusually dependent on the flow rates. In previous figure the saturated oxygen concentration of 0.1689mM(5.4ppm), at 25°C, was used for the computation. In comparison, Fig. 4 the employed oxygen concentrations are three different values : 0.08445(2.7ppm), 0.1689(5.4ppm), and 0.3378mM(9.5ppm). These values were selected based on the fact that concentrations cover the under- and super-saturated oxygen levels in the reactor inlet. There are several reported applications¹⁴ of oxygen super-saturation, generated by the decomposing hydrogen peroxide in a bio-reactor in order to supply ample amount of the much needed oxygen to microorganisms. Plots of the dimensionless oxygen concentration vs. the dimensionless reactor length, at the flow rate of 1.50mL/s, were shown in the figure. Higher conversion at the reaction rate is approaching the maximum rate, V_m . Note that the oxygen concentration is larger than the K_m value of 0.169mM(see Table 1), and the zero-order rate is carried out by the immobilized enzyme at the oxygen level. Similarly, at the lowest

oxygen concentration of 0.08445mM, the rate was significantly retarded, since at this concentration, the rate was presumably taking place in the first-order. In Fig. 5, similar plots of the fractional conversion of oxygen against the flow rates were presented using the same three different oxygen concentrations. Again, the highest conversions are seen from the plot at the higher oxygen concentrations, and the longer residence time(lower flow rates). Even at the lowest flow rates, poor conversion of not more than 82% of the lowest oxygen concentration of 0.08445mM is seen from the plots. This result further confirms the computational results from Fig. 4 and the magnitude of the substrate concentrations, generally, in the enzyme catalysis. Fig. 5 depicts an overall trend of higher flow rates reducing contact time between the reactants and the catalytic surface of the immobilized tyrosinase and a lower conversion of the phenols and oxygen (although the extent of the reduced conversion is much less with higher oxygen concentration).

4.3. Qualitative analysis on phenol removal by the enzyme

The phenols represent one of the most important classes of synthetic industrial chemicals and are widely used in many industries. Because of this use, they are often found in the effluent streams of many process industries. Studies¹⁻⁴ have been made in the past concerning phenol oxidation by the enzyme tyrosinase as an effluent way for the phenol removal from contaminate waste.

Since the ultimate propose of the tyrosinase application would be the removal of the phenols and not the oxygen from the waste stream, it may be of interest to know how much of the phenol is removed as the oxygen is consumed. Sun *et al.*² performed a qualitative kinetic model of phenol oxidation by the tyrosinase in order to estimate the amount of oxygen consumed as the enzymatic oxidation of the phenols proceeded. In their study, the first reaction considered was the catalytic reaction by

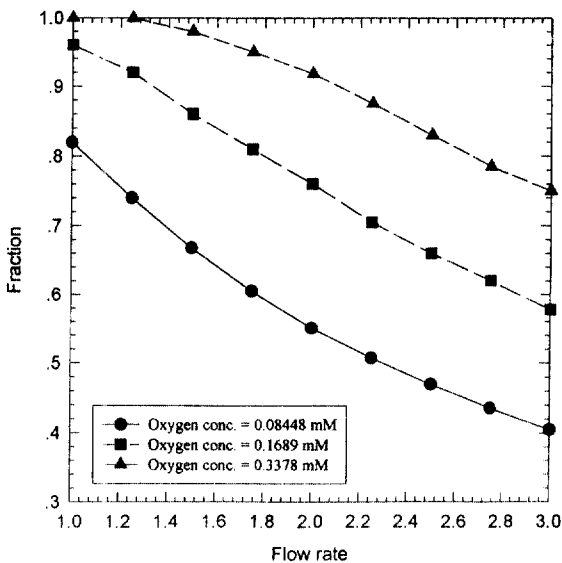


Fig. 5. The fraction along the catalytic bed at three different oxygen concentration.

tyrosinase, where one atom of molecular oxygen was incorporated into the aromatic structure, and the reducing agent AH_2 was oxidized through a chemical reaction named monooxygenation occurs. In this reaction, tyrosinase also served as a catalyst for the second reaction: the oxidation of *ortho*-diphenol to *ortho*-quinone. They used chitosan as the sorbent for *ortho*-quinone. The kinetic model showed in Fig. 2 where the monophenol is converted to *ortho*-diphenol at rate, r_1 , the *ortho*-diphenol is converted to *ortho*-quinone at r_2 , and the *ortho*-quinone is converted at r_3 . The relative rate is proposed such that the rate, r_1 , is much less than r_2 and r_3 . Therefore, the first oxidation step was the rate-limiting step, and the monophenols were chemisorbed as soon as they were oxidized. From the result, a stoichiometric table was created for the oxygen and phenol reaction.

At flow rate 1.00mL/s, the oxygen conversion is 0.9612. At this conversion, the concentration of oxygen is much less than the concentration of phenol. It can, therefore, be thought of as remaining almost constant throughout the reactor. Only 0.29% conversion of phenol was achieved.

4.4. Comparison between axial dispersion and plug flow model

In order to compare to the substrate conversion by the plug-flow and dispersion models, equation (5) was solved two different situations: the plug-flow model, D_{ax} was set to zero, and for the dispersion model, the original equation was retained for the solutions. Result of computation showed no significant difference between the two models.

The computational results are shown in Fig. 6. In Fig. 6, the dimensionless oxygen concentration vs. the dimensionless time is plotted. Surprisingly, the exit concentrations of the axial dispersion and PFR models showed the same conversions under identical reactor conditions. This result suggests that the behavior of the immobilized enzyme can be satisfactorily analyzed either by the PFR or the

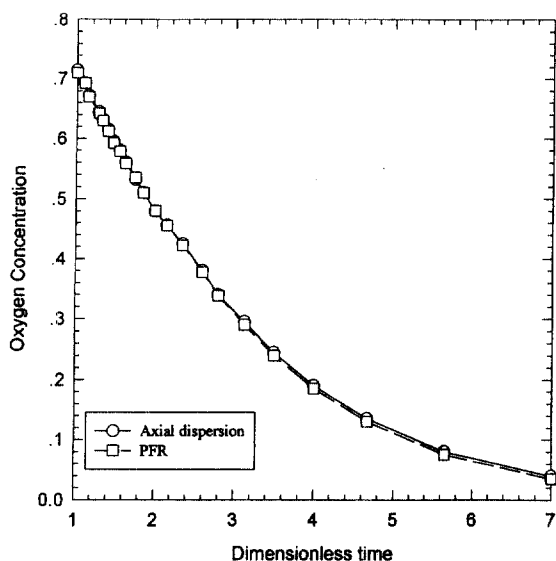


Fig. 6. Time course of the oxygen concentration change in the packed-bed by axial dispersion and plug flow models.

dispersion models. The result is in conformance with the previous results obtained by Kobayashi and Moo-Young¹⁵ and Fogler.¹⁶ Kobayashi and Moo-Young¹⁵ reported that the presence of the dispersion has no adverse effects on the conversion of the substrate in the zero-order regime of the Michaelis-Menten kinetics for the immobilized enzyme reactor. Fogler¹⁶ obtained a similar result, but the substrate conversion was slightly lower with the dispersion model for the first-order regime of the Michaelis-Menten kinetics. In both studies, only the theoretical study was presented with no experimental verification.

The result of this study, completely agree with those of Kobayashi and Moo-Young and Fogler. Our results appear to be slightly closer to the results of the zero-order results of the Michaelis-Menten regime done by Kobayashi and Moo-Young.

5. Conclusion

The effects of the external and internal mass transfer resistances were studied for a system of

immobilized tyrosinase on activated carbon. A 2.54cm diameter and 10cm long packed-bed catalytic reactor and immobilized tyrosinase on activated carbon were employed in this study for the simultaneous conversion of phenol and oxygen.

The Biot number argument was introduced in comparing the importance of the external mass transfer and the internal diffusional resistance. A typical Biot number of 64.25 was found in this study suggesting the importance of the internal diffusional resistance over the external resistance. This number is considerably larger than reported literature numbers, further confirming the negligible external mass transfer resistance. Once the importance of the internal diffusional resistance was identified, the Damkohler number was introduced to confirm the reaction rate as being a rate-limiting step. After these comparisons were made, it was possible for the study to focus on the effectiveness factors and the Thiele's modules. Finally, the effect of the dispersion model was introduced to see the influence of the dispersion on the phenol conversion by the immobilized tyrosinase. The resulting differential equations from the dispersion model were solved numerically. Satisfactory computational results were obtained from the model equations. When the dispersion model was compared with the plug-flow model, no significant difference was noted in the computational outputs, which is in complete agreement with the previously reported results. Therefore, the immobilized tyrosinase reactor can be satisfactorily analyzed by using the plug-flow model.

감사의 글

이 논문은 1996학년도 청주대학교의 학술연구조성비(특별과제)에 의하여 연구되었으며 이에 감사드립니다.

Nomenclature

D_a Damkolher number

D_{fr}	Fluid radial mass effective dispersion coefficient
D_{fa}	Fluid axial mass effective dispersion coefficient
e_0	Concentration of total amount of enzyme
E_{OX}	Fully oxidized form of enzyme
E_r	Fully reduced form of enzyme
k_c	Mass transfer coefficient
K_m, K_m^*	Michaelis-Menten constant
K_m^0	Apparent Michaelis-Menten constant
P	Product
P_e	Peclet number
R_T	Reaction rate
r	Position on radial dimension
S	Dimensionless concentration
S_A	Concentration of substrate A
S_B	Concentration of substrate B
S_{A0}	Bulk concentration of substrate A
S_{B0}	Bulk concentration of substrate B
u_i	Fluid interstitial velocity
V_f	Fluid volume
V_s	Solid catalyst volume
V_m^0	Apparent maximum reaction rate
V_m, V_m^*	Maximum reaction rate
z	Axial coordinate

Greek symbols

ϵ	Void fraction of reactor volume
η	Effectiveness factor
λ	Dimensionless position

References

1. A. Golan-Goldhirsh and J. R. Whitaker, *Adv. Exp. Med. Biol.*, **177**, 437(1984).
2. W. Sun, G. F. Payne, M. S. G. L. Moas, J. H. Chu, and K. K. Wallace, *Biotechnol. Pro.*, **8**(3), 179(1992).
3. D. F. Healy and K. G. Strothkamp, *Arch. Biochem. Biophys.*, **211**(1), 86(1981).
4. P. D. Aldridge and J. R. A. Walker, *Mauri Ora*, **8**, 53(1980).
5. H. S. Mason, *Nature*, **177**, 79(1956).
6. J. E. Bailey and D. F. Ollis, "Biochemical Engineering Fundamental", 2nd. Ed., Macgraw-Hill, New York, U. S. A., 1986.
7. Q. H. Gibson, B. E. P. Swoboda, and V. Massey, *Biology. Chem.*, **11**, 3927(1964).

8. T. Nakamura and Y. Ogura, *J. Biochem.* (Tokyo), **52**, 214(1962).
9. F. R. Duke, *JACS.*, **91**, 3904(1969).
10. Y. K. Cho, Ph. D. Dissertation, Univ. of Houston, Texas, 1977.
11. H. A. C. Montgomery, N. S. Thom, and A. Cockburn, *Appl. Chem. J.*, **14**, 280(1964).
12. T. H. Chilton, A. P. Colburn, and E. I. De Pont de Nemours, *Ind. Eng. Chem.*, **26**, 1183(1934).
13. L. Goldstein and G. Manecke, "The chemistry of enzyme immobilization", Applied Biochemistry and Bioengineering, Vol 1, L. B. Wingard, E. Katchalski-Katzir, and L. Goldstein, Ed., Academic Press, New York, 1976.
14. G. F. Format and K. B. Bischoff, "Chemical Reactor Analysis and Design", 2nd. Ed., John Wiley and Sons, New York, U. S. A., 1990.
15. T. Kobayashi, and M. Moo-Young, *Biotechnol. Bioeng.*, **13**, 893(1971).
16. H. S. Fogler, "Elements of Chemical Reaction Engineering", 2nd. Ed., Prentice Hall, Englewood Cliffs, New York, U. S. A., 1991.